Supporting Information for

Fabrication of High Performance $ZnIn_2S_4$/Si Heterostructure Photodetector Array for Weak Signal Detection

Zhaoqiang Zheng[1], Jiandong Yao[2], Weijia Li[2], Le Huang[1], Ye Xiao[1], Zhongfei Mu[3], Guowei Yang[2*], Jingbo Li[1, 4, 5*]

[1] School of Materials and Energy, Guangdong University of Technology, Guangzhou, 510006, Guangdong, P. R. China.

[2] State Key Laboratory of Optoelectronic Materials and Technologies, Nanotechnology Research Center, School of Materials Science & Engineering, Sun Yat-sen University, Guangzhou, 510275, Guangdong, P. R. China.

[3] Experimental Teaching Department, Guangdong University of Technology, Guangzhou, 510006, Guangdong, P. R. China.

[4] State Key Laboratory for Superlattices and Microstructures, Institute of Semiconductors, Chinese Academy of Sciences, Beijing, 100083, P. R. China.

[5] State key Laboratory of Precision Electronics Manufacturing Technology and Equipment, Guangdong University of Technology, Guangzhou, 510006, Guangdong, P. R. China.

*Corresponding authors: stsygw@mail.sysu.edu.cn and jbli@semi.ac.cn

Table S1. The calculated effective masses.

	K direction	M direction
m_e^* (m_0)	0.259	0.259
m_h^* (m_0)	0.333	0.358

Figure S1. EDS spectrum of the $ZnIn_2S_4$ nanosheets.

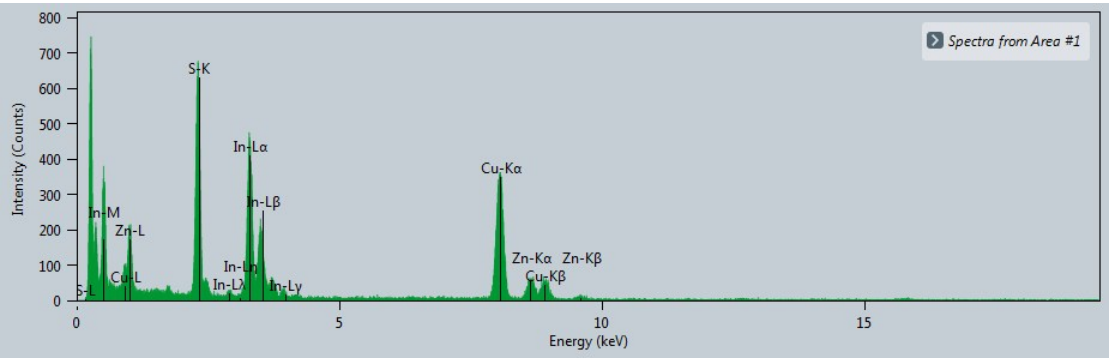

Figure S2. (a) AFM image, (b) high resolution AFM image, and (c) the height profile of the blue line in (b).

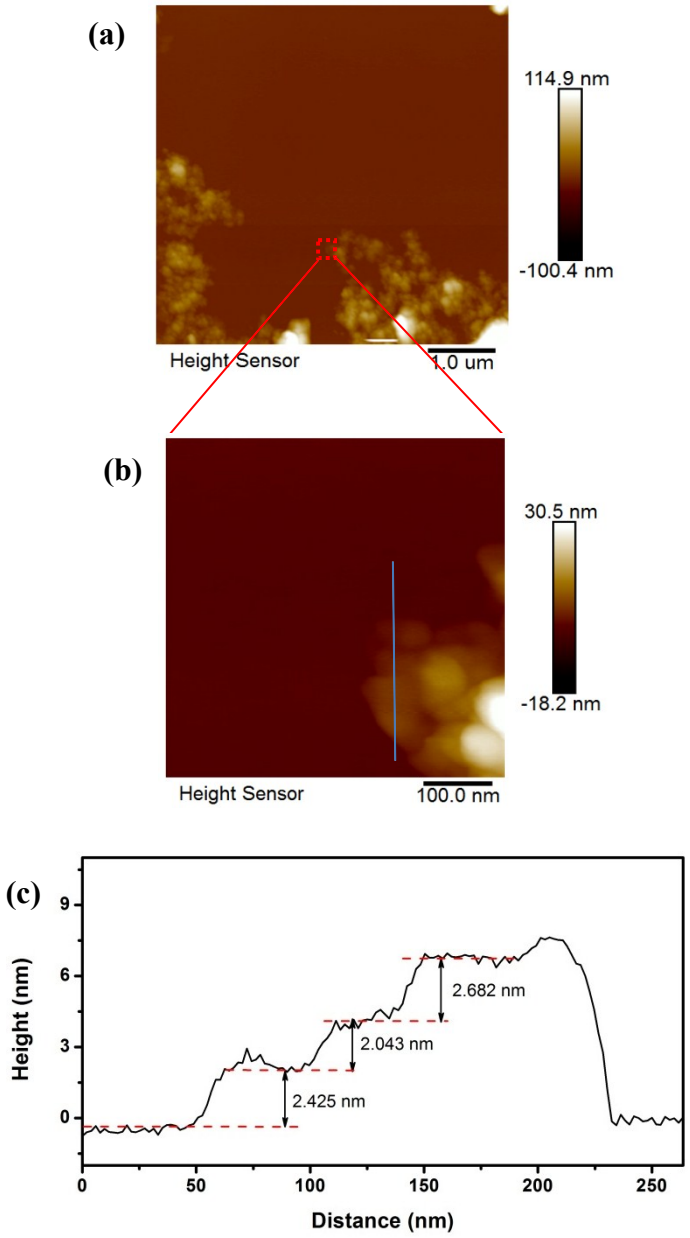

Figure S3. Survey XPS spectrum of the as-prepared $ZnIn_2S_4$ nanosheets.

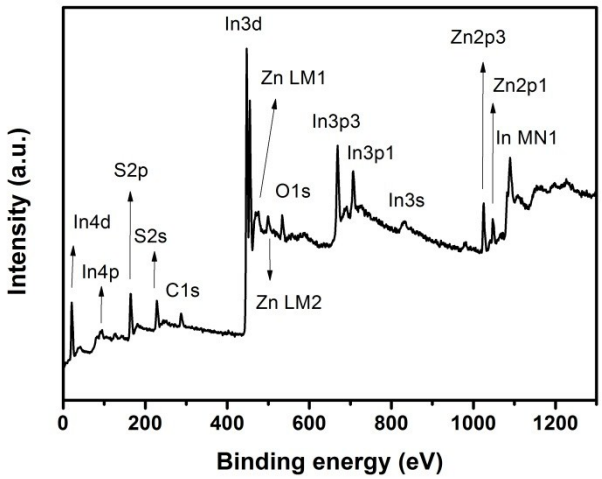

Figure S4. Schematic diagrams showing the fabrication process of the $ZnIn_2S_4$/Si heterostructure photodetector array.

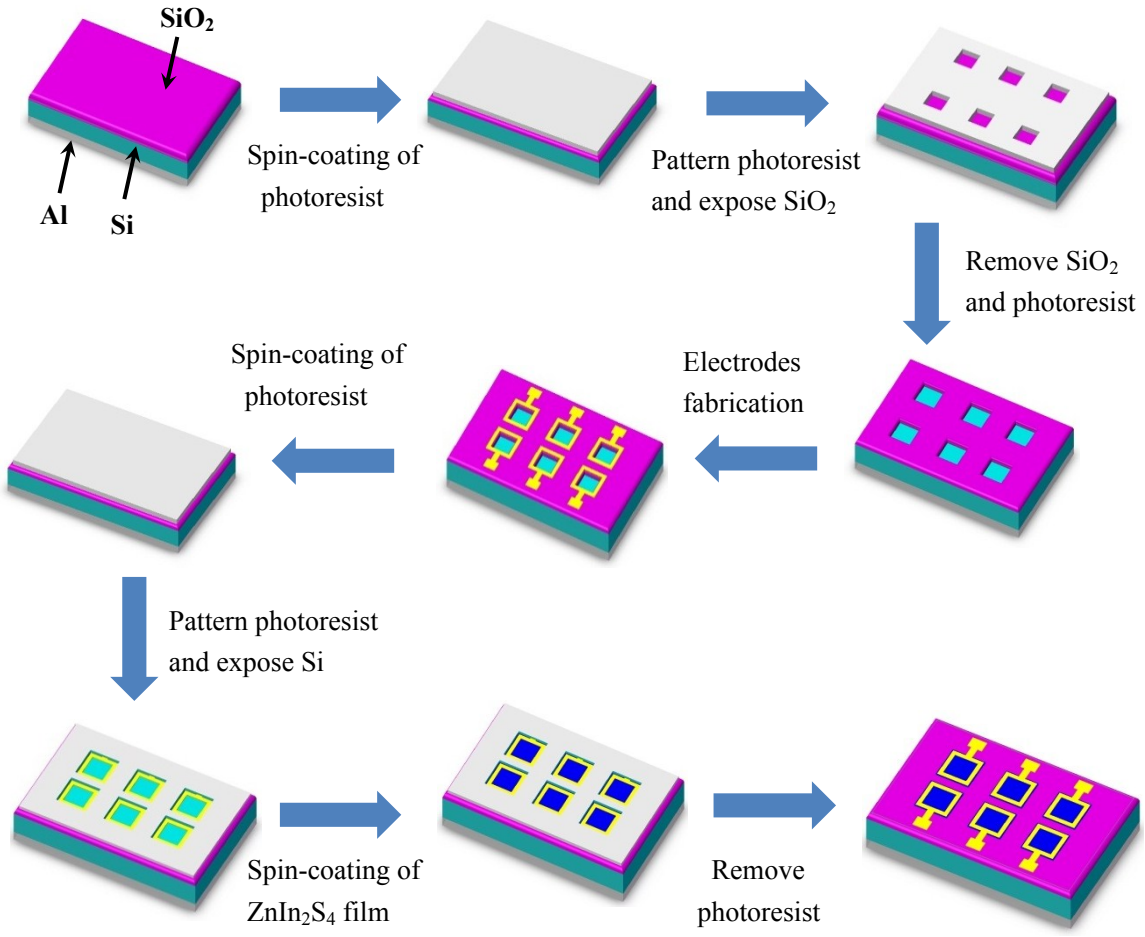

Figure S5. AFM image of the $ZnIn_2S_4$ film on the Si substrate. Inset shows the height profile along the green line.

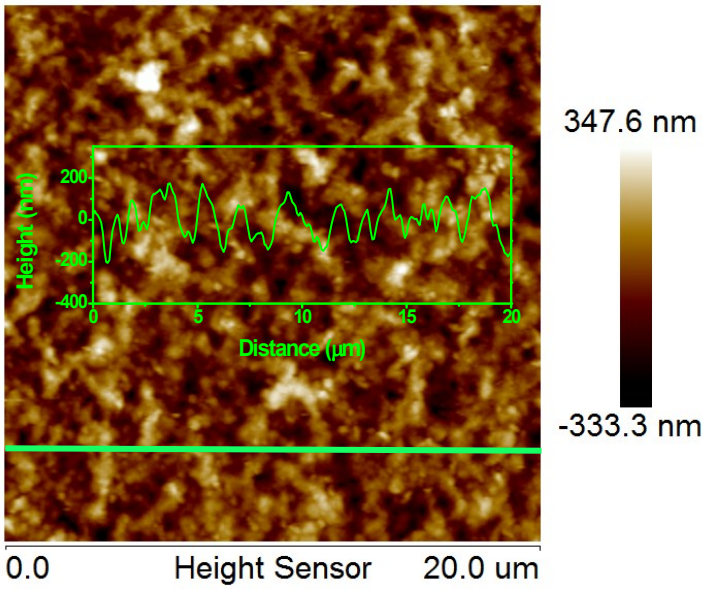

Figure S6. (a) AFM topography around the $ZnIn_2S_4$/Si heterostructure. Inset is the line-scan profile (green dash line) and the extracted height profile of $ZnIn_2S_4$ film (green solid line). (b) The SPD distribution around the $ZnIn_2S_4$/Si heterostructure. (c) SPD profile along the blue line in panel (b).

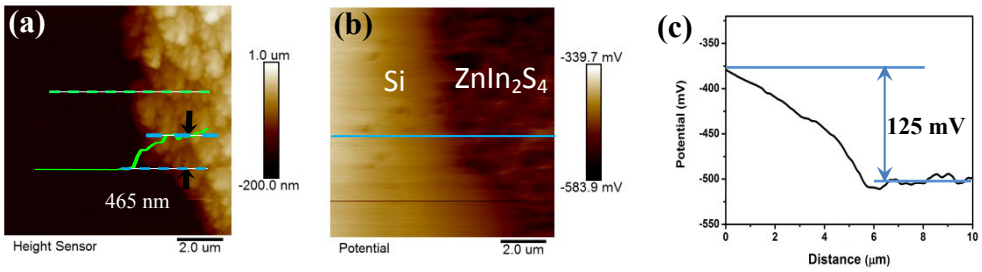

Figure S7. KPFM combined with UPS measurement to evaluate the work function of $ZnIn_2S_4$. (a) AFM surface topography image of the Au film which was deposited by electron beam evaporation. (b) The SPD distribution of the Au film with a SPD profile along the green line (inset). The mean SPD (SPD_{Au}) is -661 mV. (c) AFM surface topography image of the $ZnIn_2S_4$ film and (d) the corresponding SPD distribution. Inset shows a SPD profile along the blue line. The mean SPD ($SPD_{ZnIn2S4}$) is -315 mV. Therefore, the Femi level distinction (ΔE_{f2}) between the Au and $ZnIn_2S_4$ can be given by: $\Delta E_{f2} = W_{Au} - W_{ZnIn2S4} = eSPD_{ZnIn2S4} - eSPD_{Au}$ = 346 meV. (e) UPS spectrum near the cutoff part of the Au film. The work function of Au film can be extracted from linear part of the cutoff to base intensity of 5.14 eV. Thus, the work function of $ZnIn_2S_4$ can be evaluated to be ~4.79 eV.

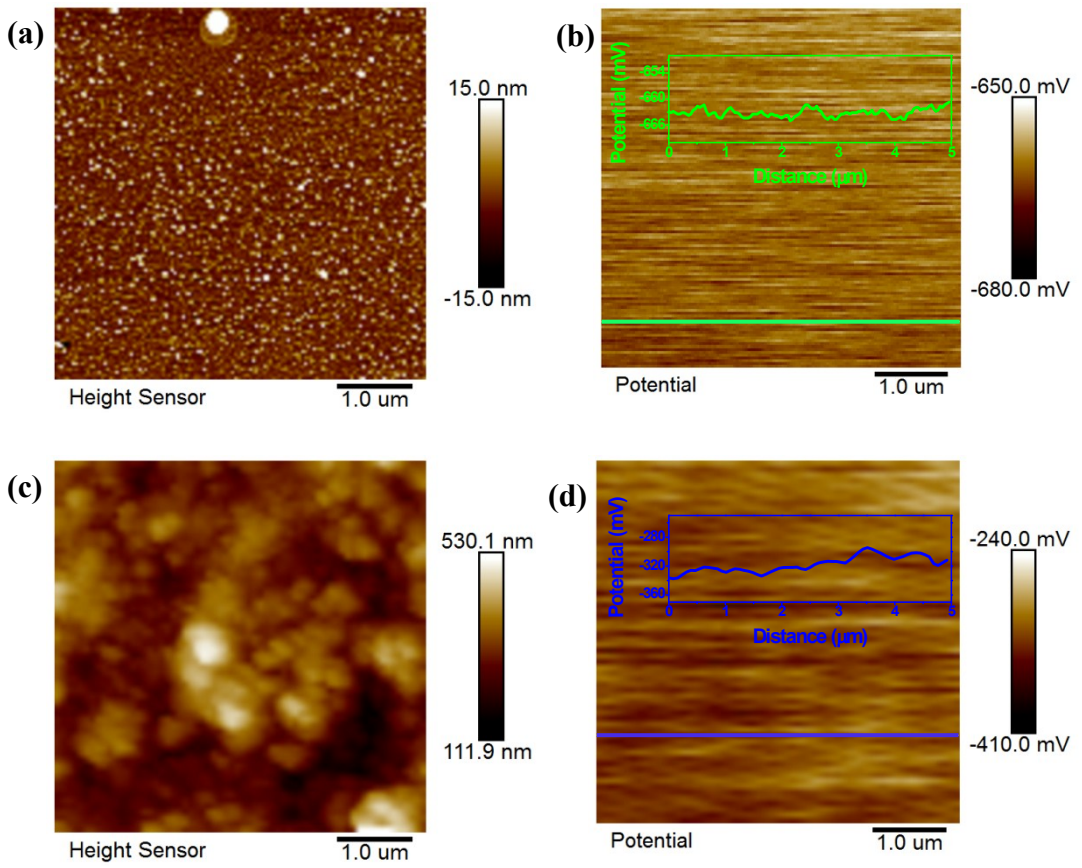

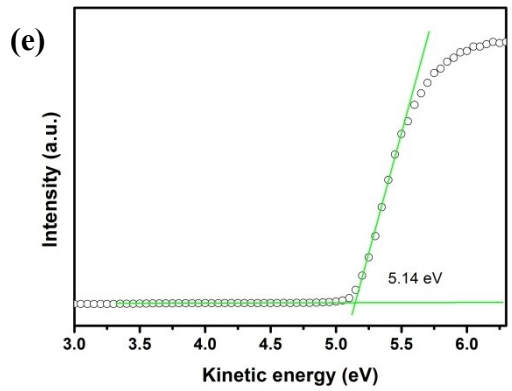

Figure S8. Valence band XPS spectrum of the $ZnIn_2S_4$ nanosheets.

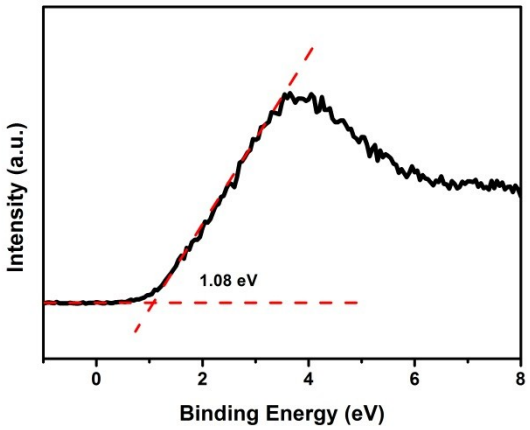

Figure S9. (a) *I-V* curve of the $ZnIn_2S_4$ photodetector in the dark. (b) The schematic description of the $ZnIn_2S_4$ photodetector.

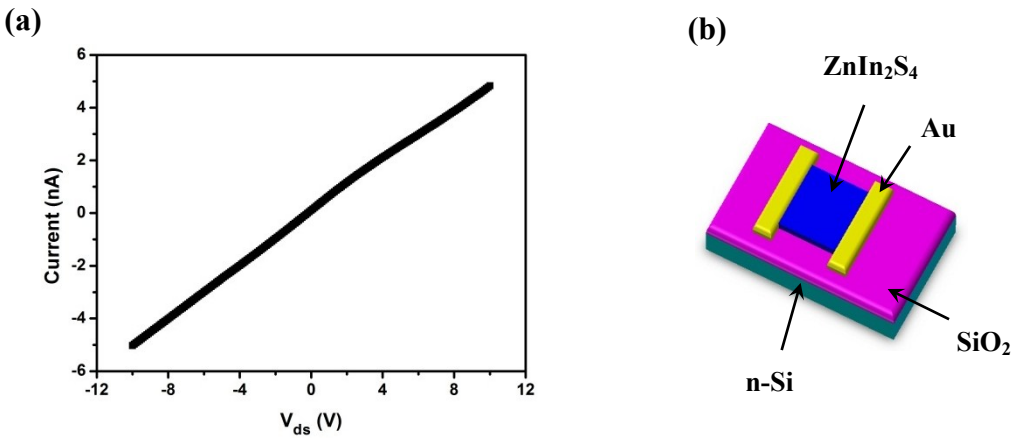

Figure S10. (a) *I-V* properties of the $ZnIn_2S_4$ photodetector under dark and 447 nm light illumination with different light intensities. (b) Responsivity as a function of light intensities of the two devices at V_{ds} =-10 V. (c) SNR (black) and specific detectivity (D*, red) as a function of light intensities of the $ZnIn_2S_4$ photodetectorat V_{ds} = -10 V. (d) Typical rise and decay behaviors of the $ZnIn_2S_4$ device measured using an oscilloscope and fitted with a single-exponential function.